

---

**Supplementary information**

---

**Skyrmion–antiskyrmion pair creation and annihilation in a cubic chiral magnet**

---

In the format provided by the authors and unedited

# Supplementary Information

## Skyrmion–antiskyrmion pair creation and annihilation in a cubic chiral magnet

Fengshan Zheng,<sup>1,2,\*</sup> Nikolai S. Kiselev,<sup>3,†</sup> Luyan Yang,<sup>1</sup> Vladyslav M. Kuchkin,<sup>3,4</sup>  
Filipp N. Rybakov,<sup>5,6</sup> Stefan Blügel,<sup>3</sup> and Rafal E. Dunin-Borkowski<sup>1</sup>

<sup>1</sup>*Ernst Ruska-Centre for Microscopy and Spectroscopy with Electrons and Peter Grünberg Institute,  
Forschungszentrum Jülich, 52425 Jülich, Germany*

<sup>2</sup>*Spin-X Institute, School of Physics and Optoelectronics,  
State Key Laboratory of Luminescent Materials and Devices,  
Guangdong-Hong Kong-Macao Joint Laboratory of Optoelectronic and Magnetic Functional Materials,  
South China University of Technology, Guangzhou 511442, China*

<sup>3</sup>*Peter Grünberg Institute and Institute for Advanced Simulation,  
Forschungszentrum Jülich and JARA, 52425 Jülich, Germany*

<sup>4</sup>*Department of Physics, RWTH Aachen University, 52056 Aachen, Germany*

<sup>5</sup>*Department of Physics and Astronomy, Uppsala University, SE-75120 Uppsala, Sweden*

<sup>6</sup>*Department of Physics, KTH-Royal Institute of Technology, SE-10691 Stockholm, Sweden*

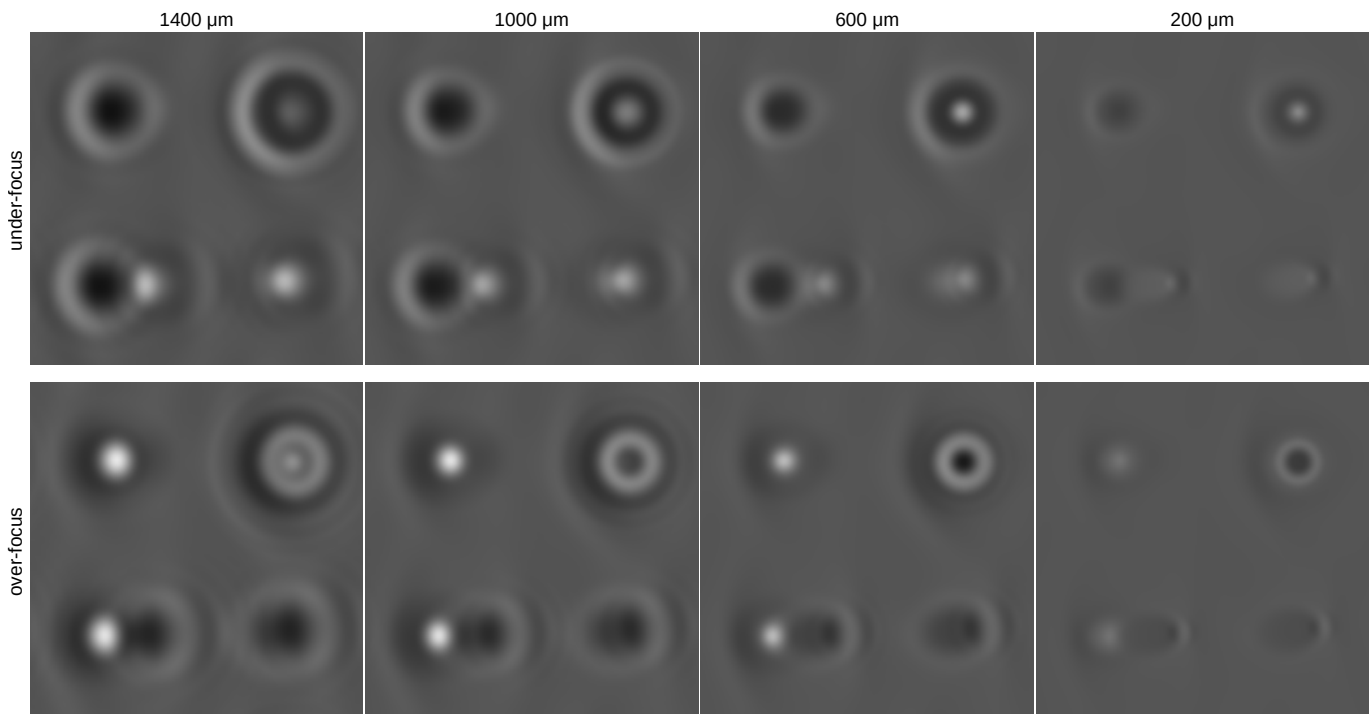


**Fig. 1 | Simulated Lorentz TEM images for a skyrmion, an antiskyrmion, a skyrmion-antiskyrmion pair and a skyrmionium for different defocus distances. For the corresponding spin texture, see Fig. 1a in the main text.**

---

\* f.zheng@fz-juelich.de

† n.kiselev@fz-juelich.de

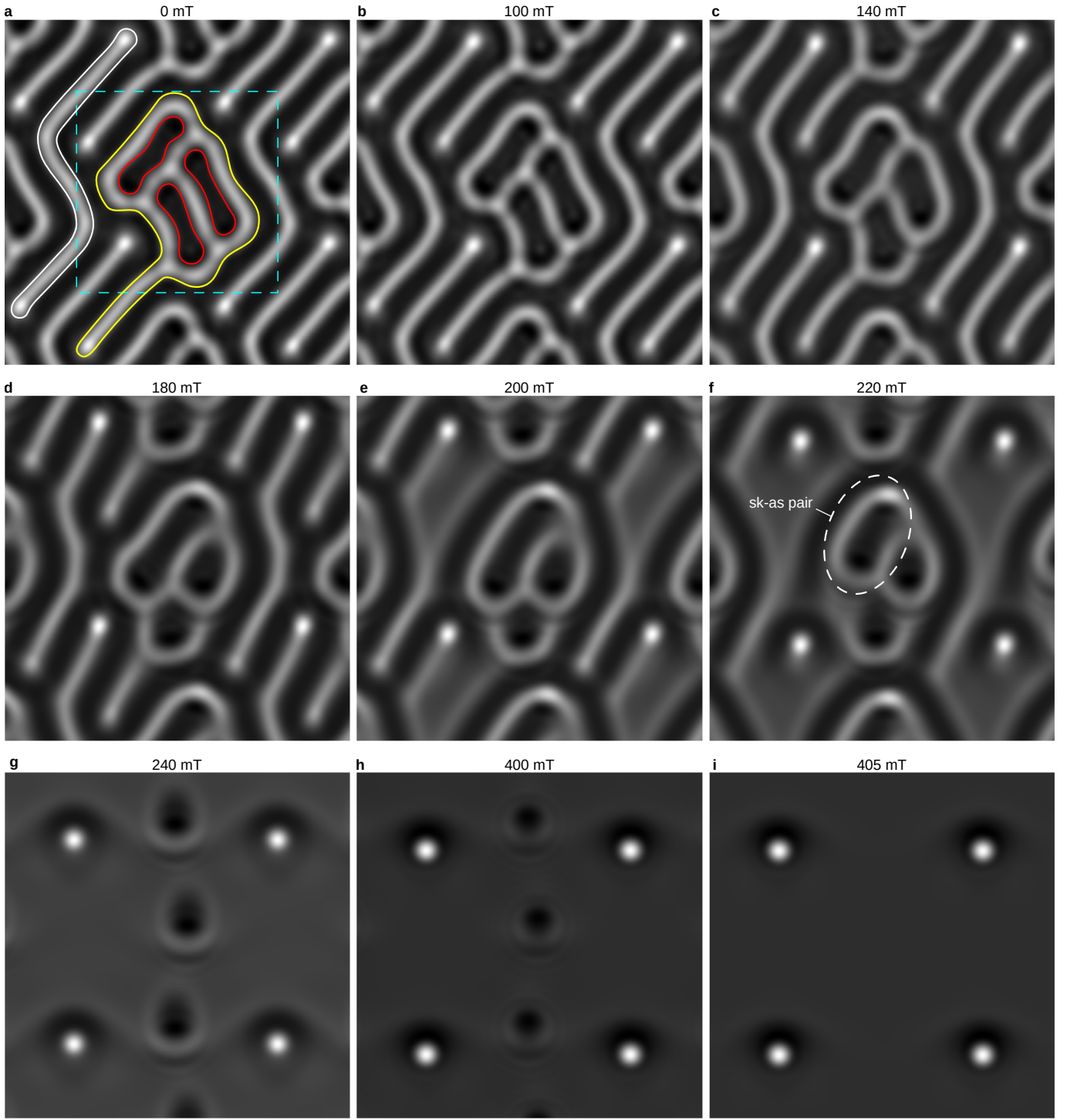


**Fig. 2 | Nucleation of antiskyrmions and skyrmion-antiskyrmion pairs in 3D micromagnetic simulations.**

Over-focus Lorentz TEM images were calculated for equilibrium magnetic textures relaxed at different values of increasing external magnetic field for a sample of thickness 50 nm, periodic boundary conditions and a defocus distance of 600  $\mu\text{m}$ . The actual size of the simulated domain is marked by a dashed blue line in **a**. For illustrative purposes, a larger field of view is shown. The white, yellow and red contour lines have the same meaning as in the experimental images shown in Fig. 3 in the main text and in **Extended Data Figs 8, 9** and **10**. As the field increases, we observe nucleation of skyrmion-antiskyrmion pairs (**f**), which quickly annihilate with further increasing external field (**g**). For a sample of thickness 50 nm, antiskyrmions collapse for  $B_{\text{ext}} > 400$  mT.

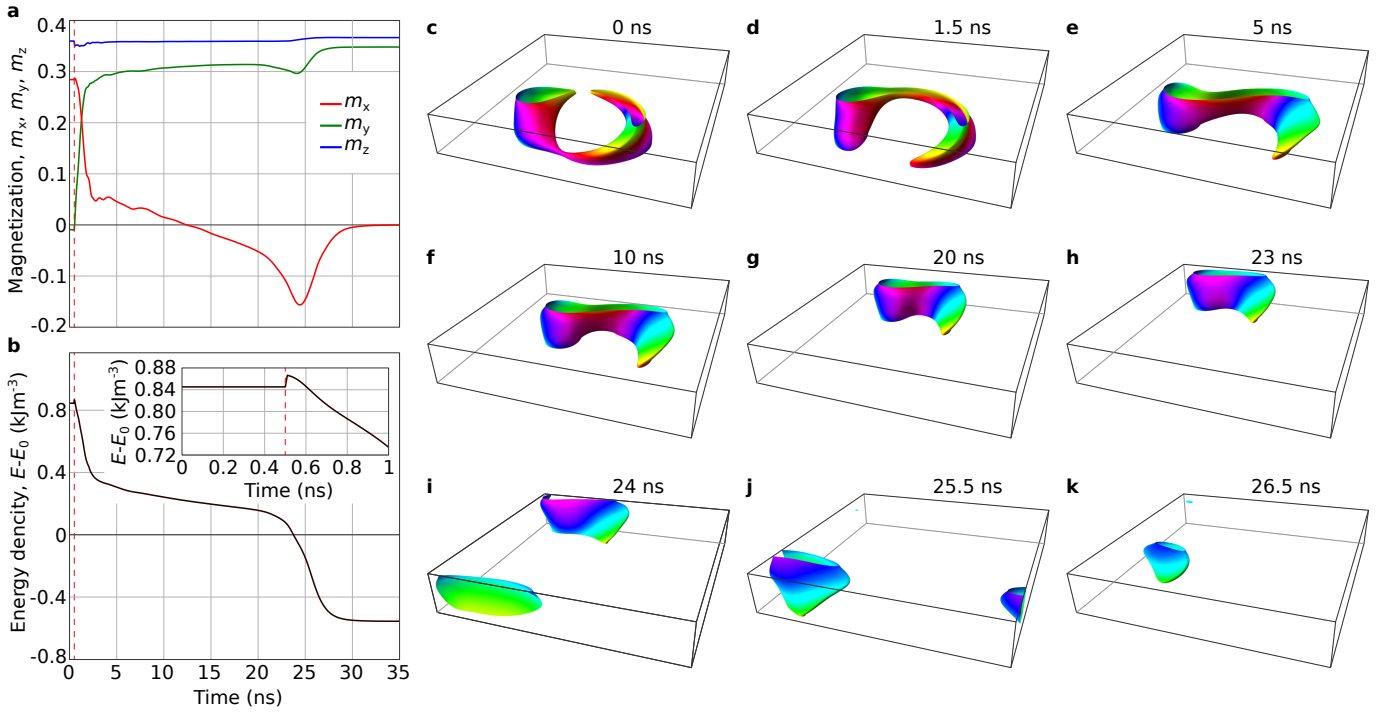


**Fig. 3 | Annihilation of a skyrmion-antiskyrmion pair in micromagnetic simulations.** The figure illustrates the results of the micromagnetic simulation based on the Landau-Lifshitz-Gilbert equation for the skyrmion-antiskyrmion pair annihilation induced by the tilt of the external field. **a** and **b** show the time dependence of the component of the averaged magnetization,  $\mathbf{m} = \langle \mathbf{M} \rangle / M_s$  and the total energy density as a function of time, respectively.  $\langle \mathbf{M} \rangle$  is the average magnetization over the volume,  $M_s$  is the saturation magnetization of the material.  $E_0$  is the energy density of the cone state at the perpendicular external field,  $B_{\text{ext}} = 250$  mT. The initial configuration in **c** was obtained by direct energy minimization. In the short-range of time between  $t = 0$  and  $0.5$  ns, the external magnetic field remains parallel to the  $z$  axis, and the energy remains fixed. At  $t = 0.5$  ns (see vertical dashed line in **a** and **b**), the field is tilted towards the  $y$  axis by  $1^\circ$ . Because the film has a nonzero in-plane component of magnetization, after the tilt of  $\mathbf{B}_{\text{ext}}$  towards the  $y$  axis, the cone phase surrounding the skyrmion-antiskyrmion pair starts to rotate around the  $z$  axis in order to align the in-plane component of magnetization to the in-plane component of the external field. This further drives the rotational motion of the antiskyrmion and initiates its fusion with the skyrmion. The images **c-k** show the snapshots of the system at different times. The magnetic configurations are presented by the isosurfaces  $m_z = 0$  as in Fig. 1 and Extended Data Fig. 3. The simulations were performed with the Mumax code. The size of the domain is the same as in Extended Data Fig. 3,  $280 \text{ nm} \times 280 \text{ nm}$  in the  $xy$  plane and  $50 \text{ nm}$  along the  $z$  axis. See Methods for material parameters and Supplementary Data 1 for the Mumax script. See Extended Data Video 1 for the real-time annihilation process.

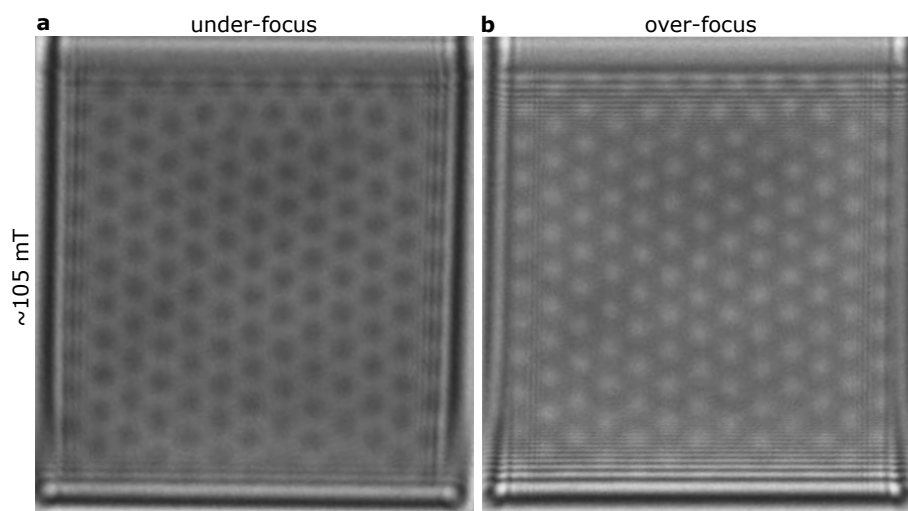


**Fig. 4** | Lorentz TEM images of the skyrmion lattice in the sample. **a** and **b** show the under- and over-focus regimes, respectively. The defocus distance is  $800 \mu\text{m}$ . The applied magnetic field is  $\sim 105 \text{ mT}$ . The images were recorded at a specimen temperature of  $250 \text{ K}$ .

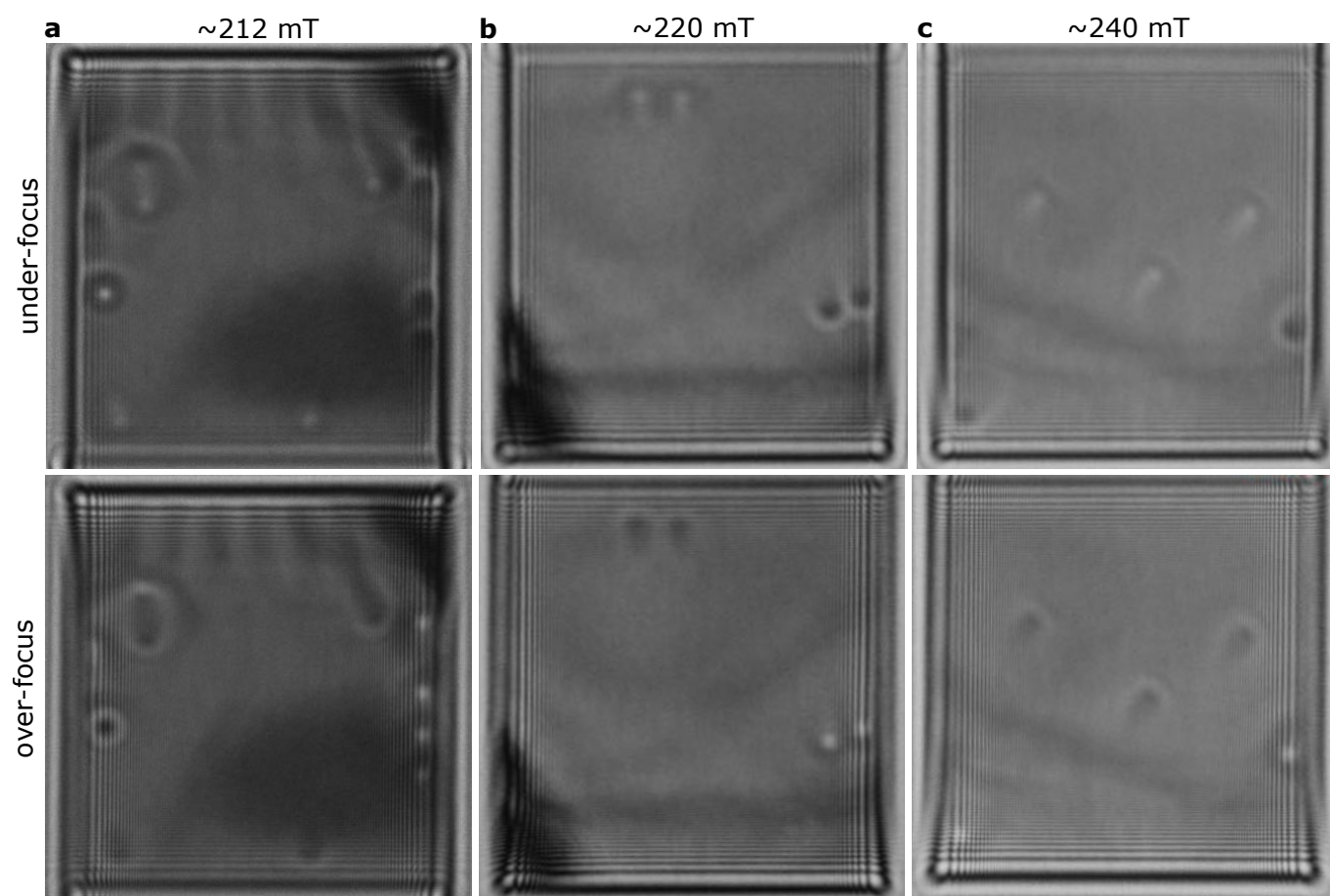


**Fig. 5** | Extended version of **Fig. 2**. Both under- and over-focus Lorentz TEM images are provided. **a-c** correspond to the magnetic states shown in Figs **2c**, **d** and **f**, respectively.

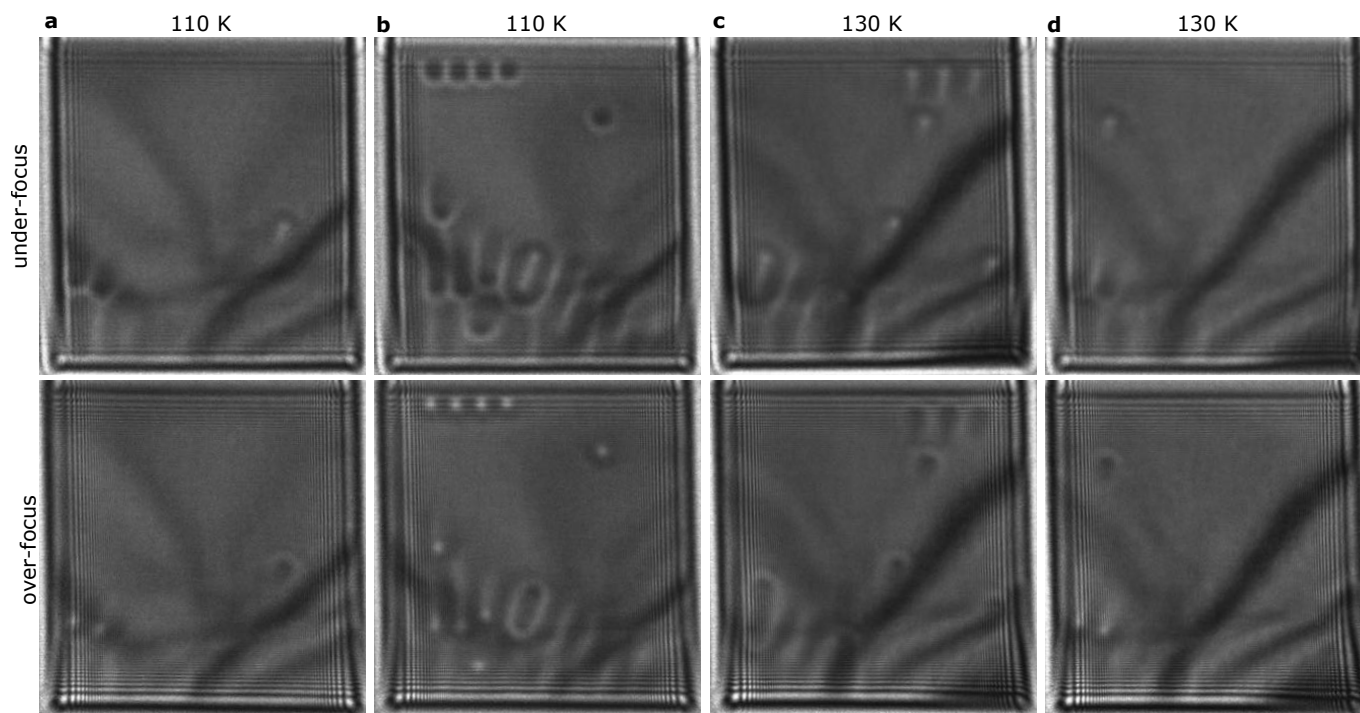


**Fig. 6 | Lorentz TEM images showing contrast features that correspond to magnetic skyrmions, anti-skyrmions and skyrmion-antiskyrmion pairs at different temperatures.** The applied magnetic field for each case was  $\sim 160$  mT. The defocus distance is  $800 \mu\text{m}$ . The specimen temperature is denoted above each panel.